Semiclassical study of avoided crossings

Toshiya Takami
Institute for Molecular Science, Myodaiji, Okazaki 444, Japan
(Received 22 March 1995)

We study the semiclassical origin of avoided crossings in nonintegrable systems with a parameter. At first, the trace formula for the stadium billiard is studied quantitatively through Fourier analysis. Then, we introduce a diabatic transformation around avoided crossings and show that the Fourier peaks after the transformation become higher for several short periodic orbits than for the original spectral density. Further, we carry out a periodic-orbit quantization to study semiclassical reproduction of avoided crossings.

PACS number(s): 05.45.+b, 03.65.Sq, 02.30.Nw, 03.65.Ge

I. INTRODUCTION

When we study the correspondence between quantum and classical systems, the notion of adiabatic invariance is important. The adiabatic invariants $\oint_{C_j} p\, dq$ play an important role in the Einstein-Brillouin-Keller (EBK) quantization condition [1]. The condition works only for systems with phase space filled by invariant tori, i.e., integrable systems. In other words, the method fails to quantize systems with stochastic regions in phase space, because the complicated structures of the phase space prevent us from detecting the invariant quantities. Even for such systems, however, it is reported that the method called *adiabatic switching* can reproduce quantum eigenvalues except in the immediate vicinity of level crossings [2]. Thus, it is desirable to complete the semiclassical study of avoided crossings in nonintegrable systems. Then, the method utilizing adiabatic invariants again acquires an ability to quantize nonintegrable systems.

For integrable systems, avoided crossings are considered to occur around resonances between tori. Since there exist no classical trajectories to connect two different tori, it is necessary to introduce imaginary trajectories, i.e., tunneling between tori. The classical resonances cause avoided crossings also in nearly integrable systems, but the avoided crossings are due to the transition-type trajectories near separatrices in the stochastic region of phase space [3].

For the strongly chaotic systems called *hard chaos,* however, the same approach cannot be applied because there exist no tori nor quantum numbers to be assigned to each of the levels. Avoided crossings arise from strong interaction between levels in quantum mechanics. To obtain semiclassical description of avoided crossings in nonintegrable systems, we must search for classical quantities to be responsible for the interaction.

In order to analyze the avoided crossings, we adopt periodic orbits as a classical quantity because of the following reasons. First, the periodic-orbit sum plays an important role in the trace formula [4,5]. Second, in scarred eigenfunctions [6–8], we can find the direct evidence for the effects of periodic orbits on eigenstates. And finally, for the systems with ergodicity, there always exist real trajectories and periodic orbits to connect any two regions in the phase space.

In a previous paper [9], we introduced a diabatic transformation for eigenvalues in the parameter variation and gave a conjecture that the avoided crossings are contributed by long periodic orbits from the Fourier analysis of the spectral density. The aim of this paper is to confirm the conjecture in the previous paper and to check how semiclassical methods work in the parameter variation of the system. To perform such investigation, we use a stadium billiard here [10]. We consider that the stadium billiard is appropriate for the present analysis, because it is one of the strongly chaotic systems with mixing and ergodicity and easy to introduce a parameter by changing the aspect ratio.

In Sec. II, we obtain explicit expression of the trace formula for the stadium billiard as a starting point for the quantitative study of the correspondence between eigenvalues and periodic orbits. Correctness of the formula is checked through Fourier analysis of the spectral density. In Sec. III, we introduce a diabatic transformation to avoided crossings in the parametric motion of eigenvalues, and we show that the height of several Fourier peaks for relatively short periodic orbits increases by the diabatic transformation. In Sec. IV, we enumerate a number of periodic orbits and try to quantize using the trace formula with the Lorentz smearing. We also check the effectiveness of the quantization procedure in reproducing avoided crossings when we change the parameter. Finally, in Sec. V we give a discussion on our result about avoided crossings and long periodic orbits.

II. TRACE FORMULA FOR A STADIUM BILLIARD

Recent quantitative studies of eigenvalues for the stadium billiard revealed the importance of *edge contributions* [11,12]. By following their methods, we obtain an expression for the trace formula in Sec. II A. The quantitative check of the formula will be done in Sec. II B through Fourier analysis of the spectral density [13].

A. Trace formula

The stadium billiard system represents motion of a particle in hard walls constructed by putting semicircles with the radius r on both sides of a $2l \times 2r$ rectangular box. This is one of the examples of a strongly chaotic system and is proven to have ergodicity and mixing [10]. Since the full stadium is symmetric with respect to the x and y axes, there are four subspaces belonging to different parities. We consider the quarter stadium with Dirichlet boundary condition on both of the outer walls and the symmetry axes for simplicity, i.e., we consider the antisymmetric subspace only. We introduce the ratio $\lambda \equiv l/r$ as a parameter. If we change it around $\lambda = 1$, the classical properties, such as Kolmogorov-Sinai (KS) entropy, etc., vary gently. Therefore, this system suits the investigation of the parameter variation within the nonintegrable region. Hereafter, unless we mention, the area of the billiard region in the quarter stadium is to be normalized as $1 + \pi/4$, i.e., the same area in the case $l = r = 1$.

Because a particle in the system moves freely in the billiard region and is reflected perfectly on the walls, we can obtain periodic orbits by considering geometrical optics in this region. There exists a family of neutral periodic orbits called bouncing ball orbits which bounce perpendicularly between the parallel straight sections of the billiard boundary (orbit 1 in Fig. 1 and its repetition). The other periodic orbits are isolated and unstable.

When we obtain the trace formula for the stadium billiard, we apply the Berry-Tabor formula [14] for the bouncing ball orbits and the Gutzwiller formula [4] for the other unstable orbits. The important points to be considered are the effect of the right angle corners and the special trajectories through connecting points of the straight boundary and the semicircles [11,12]. If we include these *edge contributions* as additional terms, the semiclassical density of states $d_{sc}(k^2)$ is represented up to the order k^{-1} by a sum of four terms: d_B (for bouncing orbits), d_I (for isolated orbits), d_E (for edge contributions), and the average density $\overline{d_0(k^2)} = \mathcal{A}/4\pi - \mathcal{L}/8\pi k$, where $\mathcal{A}$ and $\mathcal{L}$ are the area and the perimeter of the billiard region, respectively.

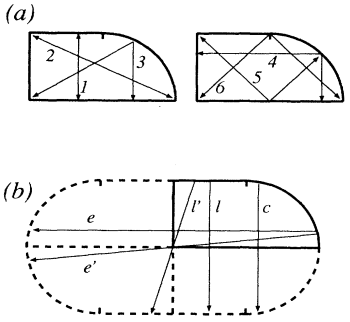

FIG. 1. (a) Several short periodic orbits in quarter stadium; (b) trajectories due to additional edge contributions (see text).

1. Bouncing ball orbits

The oscillatory part of the semiclassical density of states is mainly contributed by the bouncing ball orbits in the semiclassical limit. A trace formula for the integrable or pseudointegrable systems [14] can be applied to the orbits. The contribution of the bouncing orbits appears in the semiclassical density of states as the oscillatory term with the order $k^{-1/2}$,

$$d_B(k^2) = \frac{1}{2\pi\sqrt{2\pi k}} \sum_{n=1}^{\infty} \frac{a_B}{\sqrt{n l_B}} \cos\left(nkl_B - \frac{\pi}{4}\right). \quad (1)$$

Here, a_B is the area of the region wiped by the bouncing orbits and l_B is the length of the orbits. In the case we consider here, i.e., the antisymmetric states, we set $a_B = 2rl$ and $l_B = 2r$.

2. Isolated orbits

For the infinitely many unstable orbits, we apply the Gutzwiller trace formula,

$$d_I(k^2) = \frac{1}{2\pi k} \sum_{\gamma} \sum_{n=1}^{\infty} A_\gamma^{(n)} \cos\left(nkl_\gamma - \frac{n\sigma_\gamma \pi}{2}\right), \quad (2)$$

where the summations are carried out over all the primitive isolated orbits γ and the repetition number n of the orbit. l_γ denotes the length of the primitive orbit, σ_γ is the Maslov index, and $A_\gamma^{(n)}$ is the amplitude factor obtained from the length and the stability exponent of n times passage of the orbit γ. The amplitude factor is represented by

$$A_\gamma^{(n)} = \frac{l_\gamma}{\sqrt{|\mathrm{tr} M_\gamma^n - 2|}},$$

where M_γ denotes the linearized Poincaré map in the vicinity of γ.

Isolated orbits are classified into two groups by its geometrical property. The orbits retracing themselves are called self-retracing orbits and we distinguish them from the other non-self-retracing ones. The non-self-retracing orbits contribute twice to the trace formula because the motion for the positive and negative directions should be treated independently, whereas the self-retracing ones contribute once because the motion is not changed even if we inverse the direction. Note that the orbits just through right angle corners should be treated as self-retracing in the quarter stadium (see Appendix A).

For several short orbits in parameter value $\lambda = 1$, we display their shapes in Fig. 1(a), and the values of $A_\gamma^{(n)}$, l_γ, and σ_γ in Table I. The orbits 6, 6′, and 6″ exist in $\lambda \geq 1$ only. At $\lambda = 1$ where pruning for the orbits just occurs, the additional numeric factor 1/2 or 1/4 is needed.

TABLE I. Characteristic quantities for short periodic orbits ($n = 1$).

Orbit	l_γ	$A_\gamma^{(1)}$	σ_γ
2	4.472	1.414	9
3	5.196	1.500	12
4	4.828	1.436	10
5	4.828	2.030	11
6	5.657	$1.414\times\frac{1}{4}$	13
$6'$	5.657	$1.414\times\frac{1}{2}$	14
$6''$	5.657	$1.414\times\frac{1}{4}$	15

3. Edge contribution

Here we consider the extra contribution from boundary edges, right angle corners, and connecting points between straight walls and semicircles. These extra terms give contribution of the same order in k as the isolated periodic orbits (Appendix A). The result is the sum of the terms

$$d_E = \frac{1}{2\pi k}\sum_{\gamma'} A_{\gamma'}\cos\left(kl_{\gamma'} - \frac{\sigma_{\gamma'}\pi}{2}\right). \tag{3}$$

The several contributed trajectories are displayed in Fig. 1(b) and the characteristic quantities are in Table II. The origin of the additional factor $1/2$ in the orbits e and e' is discussed in Refs. [15,16].

Summing up all contributions to the density of states, we obtain

$$d_{\rm sc}(k^2) = \overline{d_0(k^2)} + \frac{1}{2\pi\sqrt{2\pi k}}\sum_n \frac{a_B}{\sqrt{nl_B}}\cos\left(nkl_{\rm B} - \frac{\pi}{4}\right) + \frac{1}{2\pi k}\sum_\gamma A_\gamma\cos\left(kl_\gamma - \frac{\sigma_\gamma\pi}{2}\right), \tag{4}$$

where both of the unstable-orbit contributions and the edge contributions are contained in the third term.

TABLE II. Characteristic quantities for trajectories related to edge contributions.

Orbit	$l_{\gamma'}$	$A_{\gamma'}$	$\sigma_{\gamma'}$
l'	2.0	0.500	2
c	2.0	0.500	1
ll	4.0	0.318	2
$ll' + l'l$	4.0	0.500	2
$l'l'$	4.0	0.159	0
cc	4.0	0.159	2
$cl + lc$	4.0	0.543	0
$cl + lc$	4.0	0.354	1
e	4.0	$1.414\times\frac{1}{2}$	5
e'	4.0	$2.000\times\frac{1}{2}$	7

B. Fourier transformation

Eigenvalues of the stadium billiard are obtained by solving the Helmholtz equation $(\Delta - k^2)\psi = 0$ in the region of the stadium with the Dirichlet boundary condition [17]. It is known that the Fourier transform of the spectral density has peaks at lengths of periodic orbits [13]. Here, we analyze the heights of the peaks in the transformed density of states through the trace formula obtained in the preceding subsection and check the effectiveness of the formula for the stadium billiard system.

Eigenvalues obtained by numerical computations are only finite fractions of the whole spectrum. If we calculate the Fourier transform of the spectral density from the finite interval, the transformed density oscillates violently. To reduce the oscillation and make the density converge, we introduce a damping factor for the Fourier transformation.

After we multiply $8\sqrt{\pi}k\ \Delta\exp(ikl - \Delta^2k^2)$, we integrate them from $k = 0$ to ∞. For the quantum density of states $d_Q(k^2)$, we obtain

$$\int_0^\infty dk\ 8\sqrt{\pi}k\Delta\exp(ikl - \Delta^2k^2)\ d_Q(k^2) = 4\sqrt{\pi}\Delta\sum_{n=1}^{\infty}\exp(ik_nl - \Delta^2k_n^2). \tag{5}$$

The Fourier transform of the semiclassical density of states is represented by shape functions $f(x)$ and $g(x)$ which are displayed in Fig. 2 (see Appendix B),

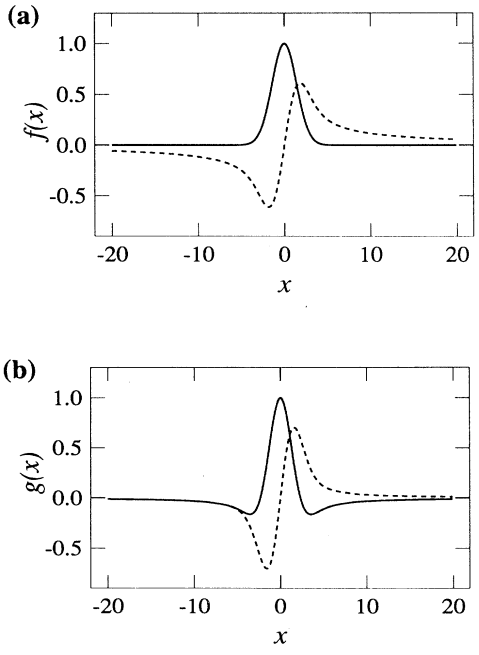

FIG. 2. The real (solid curves) and the imaginary part (dotted curves) of the line-shape functions for Fourier peaks.

$$\int_0^\infty dk\ 8\sqrt{\pi}k\Delta \exp(ikl - \Delta^2 k^2)\ d_{sc}(k^2) = \left(\frac{\mathcal{A}}{i}\frac{\partial}{\partial l} - \frac{\mathcal{L}}{2}\right) f\left(\tfrac{l}{\Delta}\right) + \frac{\Gamma(3/4)\ e^{\pi i/4}}{\pi\sqrt{2\Delta}} \sum_{m=0}^{\infty} \frac{a_B}{\sqrt{nl_B}}\ g\left(\tfrac{l-nl_B}{\Delta}\right) + \sum_\gamma A_\gamma\ e^{\sigma_\gamma \pi i/2}\ f\left(\tfrac{l-l_\gamma}{\Delta}\right). \quad (6)$$

In Fig. 3, we compare the Fourier transform of the quantum spectral density (5) (solid curves) with that of the semiclassical density (6) (dotted curves) which is obtained from the information of the classical periodic orbits. Figures 3(a), 3(b), and 3(c) are a comparison of real parts, imaginary parts, and the absolute values, respectively. All these figures are obtained by setting the damping factor $\Delta = 0.035$. And the first 1375 eigenvalues in the antisymmetric subspace for $\lambda = 1$ stadium are used to calculate the quantum curves.

In the figures, we can find excellent agreement between the quantum and the semiclassical results. Within the Fourier analysis of the spectral density, the trace formula describes the eigenvalue properties of the stadium billiard. This agreement guarantees the semiclassical investigation of the stadium billiard through the trace formula with the periodic-orbit sum.

III. DIABATIC TRANSFORMATION

As was seen in the preceding section, the periodic-orbit theory using the trace formula shows good agreement with the quantum calculation. But it is not clear how the agreement would be seen in the parameter variation of the nonintegrable systems [18] because there exist many avoided crossings due to the absence of the constance of motion other than the energy.

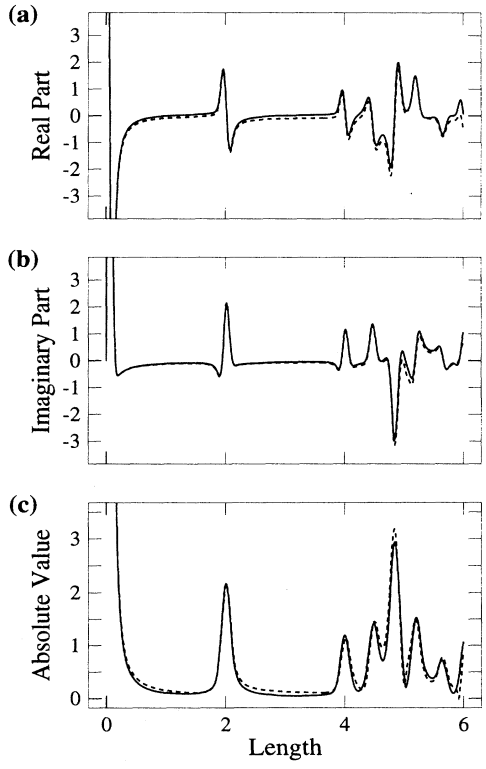

FIG. 3. Comparison of Fourier transformation of the spectral density (solid curves) and the semiclassical result (dotted curves): (a) real part; (b) imaginary part; (c) absolute value.

The aim of this section is to study the role of avoided crossings in the trace formula. Along the lines of our previous paper [9], we introduce the diabatic transformation [19] around an avoided crossing, and consider the relation of avoided crossings and long periodic orbits through the Fourier analysis of the spectral density.

A. Definition

We can see the characteristics of eigenfunctions alternating between two energy levels when the parameter goes over the region of an avoided crossing [9]. Namely, the invariant characteristics in eigenfunctions related to classical quantities are carried along diabatic lines rather than along adiabatic levels. Thus, we can expect that the quantum classical correspondence is considered to become clear when we study the system in the diabatic representation. In order to clarify such features, we introduce a two-level diabatic transformation.

The Hamiltonian around an avoided crossing is approximately represented by a 2×2 matrix,

$$H_{\text{approx}} = \begin{pmatrix} a(\lambda) & \Delta/2 \\ \Delta/2 & b(\lambda) \end{pmatrix}, \quad (7)$$

where Δ is constant. To decide the representation, we introduce another condition: diagonal elements $a(\lambda)$ and $b(\lambda)$ cross at $\lambda = \lambda_0$ where the difference between upper and lower eigenvalues has the smallest value $\Delta \equiv E_+(\lambda_0) - E_-(\lambda_0)$. Then, we get the explicit form of the transformation,

$$\begin{pmatrix} a(\lambda) & \Delta/2 \\ \Delta/2 & b(\lambda) \end{pmatrix} = \mathbf{P}(\lambda) \begin{pmatrix} E_+(\lambda) & 0 \\ 0 & E_-(\lambda) \end{pmatrix} \mathbf{P}(\lambda)^{-1}, \quad (8)$$

where

$$\mathbf{P}(\lambda) = \frac{1}{\sqrt{2}} \begin{pmatrix} \sqrt{1+S(\lambda)} & -\sqrt{1-S(\lambda)} \\ \sqrt{1-S(\lambda)} & \sqrt{1+S(\lambda)} \end{pmatrix}, \quad (9)$$

$$S(\lambda) = \text{sgn}(\lambda_0 - \lambda)\sqrt{1 - \left(\frac{\Delta}{E_+(\lambda) - E_-(\lambda)}\right)^2}. \quad (10)$$

The new bases are also represented by a linear combination of the eigenfunctions and the features of the scar are recovered by the transformation [9].

Since the energy diagram of chaotic systems is full of avoided crossings, we must extend the diabatic transformation for the multilevel case. Our strategy in the

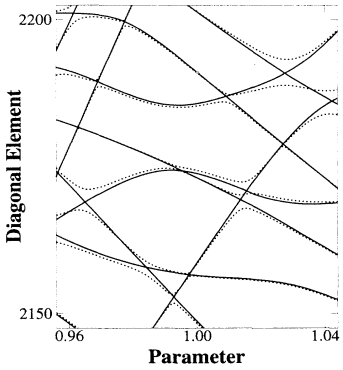

FIG. 4. Diagonal elements of Hamiltonian after successive application of the diabatic transformation (solid curves), compared to the eigenvalues (dotted curves).

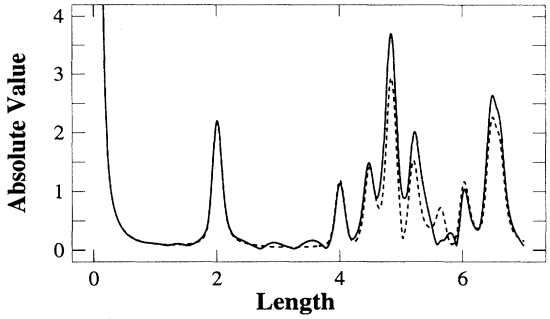

FIG. 5. Fourier transformation for density of diagonal elements in the diabatic representation (solid curve), compared with that of eigenvalues (dotted curve). Both curves are calculated for $\lambda = 1.0$.

present calculation is to apply the two-level diabatic transformation successively in the increasing order of the energy gap size of the avoided crossing, where we regard a local minima of energy differences in the parameter variation as an avoided crossing. We carry out the following procedure repeatedly: we search for a pair of levels with the smallest avoided crossing in diagonal elements on the present representation of the Hamiltonian and apply the two-level transformation (8) to the pair over a certain parameter interval.

The energy diagram of chaotic systems contains avoided crossings with various size. When they are transformed according to the above method, we find larger structures in the energy diagram, i.e., avoided crossings between distant levels other than nearest neighbors. We must decide when we should stop the procedure, because we can always find a larger one after the transformation of an avoided crossing in the limit $\hbar \to 0$. In the present calculation, we stopped the iteration when the smallest gap comes up to the size of the mean level spacings. The result for the stadium billiard is shown in Fig. 4. The diagonal elements after the transformation (solid curve) are compared with the eigenvalues (dotted curve).

B. Spectral density in diabatic representation

We have obtained the diabatic representation of the Hamiltonian of the stadium billiard in Sec. III A. The diagonal elements in this representation are considered as the eigenvalues in the diabatic approximation of the original system. Here, we analyze the spectral density of the approximate Hamiltonian through the Fourier transformation and try to interpret the diabatic approximation.

Figure 5 is the plot of the Fourier transform of the spectral density for the diagonal elements in the diabatic representation (solid curve), which is compared with that of the eigenvalues (dotted curve). It is apparent that some of the peaks for diagonal elements are higher than those for the eigenvalues.

The peaks found in Fig. 5 are the ones corresponding to some of the shortest periodic orbits. Since the total amounts of the spectral weight are not changed by the diabatic transformation, the increase of the weight in Fig. 5 indicates the relative decrease of the weight in the region of larger length. Thus, the diabatic approximation reduces the spectral weight on longer periodic orbits. In other words, the spectral weight of longer periodic orbits comes from the existence of avoided crossings. From this relation, we conclude that the origin of avoided crossings is the longer periodic orbits. This is one of the main results in this paper.

IV. SEMICLASSICAL QUANTIZATION

So far in this paper, we have analyzed quantum energy levels and extracted classical information from them. Conversely in this section, we construct eigenvalues of the stadium billiard from the information of classical periodic orbits. Moreover, we study the convergence of Gutzwiller's trace formula for the stadium billiard, and check whether the semiclassical method is powerful enough to reproduce avoided crossings.

One of the crucial problems incidental to the periodic-orbit quantization is the exponential proliferation of periodic orbits in nonintegrable systems. This leads to the difficulty of convergence of the trace formula. In order to ward off the difficulty, we use the Lorentzian smearing version of the trace formula.

A. Classical periodic orbits

Semiclassical quantization by the trace formula has been studied in several systems. Since we can obtain periodic orbits by geometrical consideration for billiard systems, the enumeration is easier than for other systems. If we find a coding rule for the periodic orbits, moreover, we can implement effective algorithms for systematic enumeration. This enables us to carry out the periodic-orbit quantization much easier. For the stadium

TABLE III. Number of primitive periodic orbits in a quarter stadium.

Length of code string	Aspect ratio 0.5	0.75	1.0	1.25	1.5
2	2	2	2	2	2
3	2	2	2	2	2
4	8	8	8	8	8
5	7	7	10	15	15
6	20	23	30	30	39
7	29	47	49	59	59
8	71	116	164	192	208
9	117	178	323	444	531
10	321	591	796	1 108	1 416
11	545	1 507	2 198	2 893	3 568
12	1 336	3 499	6 340	9 053	10 783
13	3 217	8 563	16 095	25 030	31 941
14	7 760	24 757	43 739	69 427	93 075

billiard, there exist two coding methods to my knowledge [20,21]. In the present calculation, we use the 6-alphabet method by Hansen [20,18].

The procedure to enumerate periodic orbits for the stadium billiard is divided into two parts. At first, we enumerate all the code strings according to the grammatical rules. It is important in this step to eliminate the code strings breaking the rules (parameter independent pruning [20]) and to reduce the redundancy according to symmetry of the stadium. In the next, we obtain orbits in the real billiard plane by performing the Newtonian method [22]. In this step, we eliminate the orbits which are grammatically correct but cannot satisfy the law of reflection (parameter dependent pruning [20]).

In Table III we show the number of periodic orbits obtained by this procedure. Figure 6 shows how the number of periodic orbits increases according to the length of the orbits. The staircaselike behavior of this figure is due to the fact that there are accumulation points of whispering-gallery orbits at $(l + \pi r)n$, where l is the length of the straight part, r is the radius of the semicircle, and n is an integer $(1, 2, \ldots)$. The effect of whispering orbits on the semiclassical quantization, however, will be comparatively small because a high cancellation is expected between orbits of almost the same length with different phase factors [11].

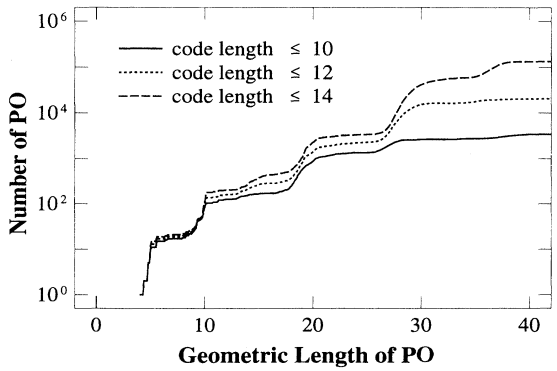

FIG. 6. Integrated number of unstable periodic orbits.

B. Semiclassical quantization

Using the Lorentz smeared version of the trace formula [5,22], we carry out the periodic-orbit quantization for a stadium billiard. The semiclassical density of states is represented by

$$d_{sc}(k^2;\varepsilon) = \pi\varepsilon\overline{d_0(k^2)} + \frac{\varepsilon l r}{\sqrt{2\pi k}}\sum_{n=1}^{\infty}\frac{\cos\left(2nkr-\frac{\pi}{4}\right)}{\sqrt{2nr}}\exp\left(-n\frac{\varepsilon r}{k}\right) + \frac{\varepsilon}{2k}\sum_{\gamma}A_\gamma\cos\left(kl_\gamma-\frac{\sigma_\gamma\pi}{2}\right)\exp\left(-\frac{\varepsilon l_\gamma}{2k}\right). \tag{11}$$

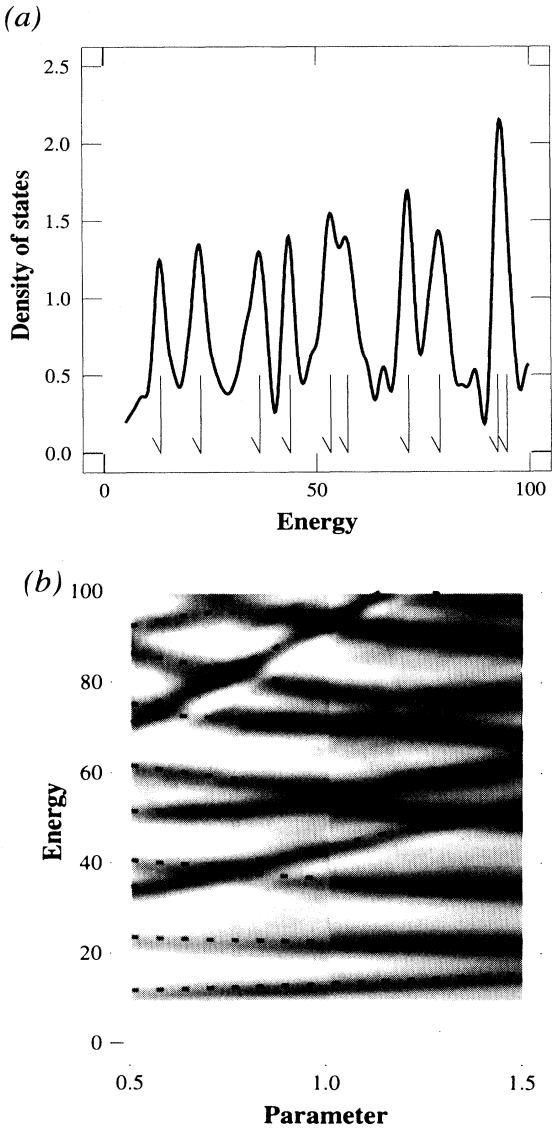

FIG. 7. (a) Semiclassical density of states for $\lambda = 1.0$. (b) Semiclassical density of states as the parameter λ is changed.

Here, the third term on the right-hand side denotes both of the contributions of isolated orbits and edges.

Convergence of the right-hand side of Eq. (11) is controlled by the smearing factor ε. For the system whose periodic orbits show almost random distribution, we can estimate the optimum value of ε from the classical information [22]. The distribution of periodic orbits of the stadium billiard cannot be considered fully random as we have seen in Sec. IV A. Thus, we could not find the method of estimation other than choosing the value of ε by rule of thumb. The result of the semiclassical quantization for $\lambda = 1.0$ and $\varepsilon = 2.5$ is displayed in Fig. 7(a). The solid curve represents the semiclassical result calculated by Eq. (11), and arrows below the curve indicate the exact eigenvalues.

Figure 7(b) shows the semiclassical density of states for various aspect ratios. The horizontal axis is the aspect ratio and the vertical axis is the energy. The dotted curves imposed on the plot represent eigenvalues obtained by the quantum mechanical calculation. As a whole, the result of the semiclassical quantization agrees with the quantum result and it seems that the reproduction of avoided crossings can be achieved by the periodic-orbit quantization (see the discussion section below).

V. SUMMARY AND DISCUSSION

In this paper, we have studied contribution of periodic orbits in the parameter variation of nonintegrable systems through the trace formula. First, we obtained the expression of the trace formula for the stadium billiard, and tested the validity through Fourier analysis of the spectral density. Next, we introduced diabatic transformation for avoided crossings in the parameter variation to study the relation between avoided crossings and long periodic orbits.

The strategy we used is to show that the diabatic approximation emphasizes short time motion, i.e., the increase of the spectral density for short periodic orbits. This implies the relation between avoided crossings and long periodic orbits since the total amounts of spectral weights do not change before and after the diabatic transformation. It may be expected from physical considerations that the diabatic approximation is related to the short time phenomena in integrable and nearly integrable systems. We showed that such a relation can be observed in the periodic orbits even if the system is fully chaotic. The next step of the analysis will be to search for the explicit periodic orbits related to an avoided crossing, i.e., we should consider the constructive method to search for such periodic orbits corresponding to the avoided crossing.

In the preceding section, we carried out the semiclassical quantization and studied the semiclassical density of states from the viewpoint of the parameter variation. Quantum mechanics is continuous when a parameter is varied, whereas classical mechanics is not continuous as we can see in the pruning of classical periodic orbits. It should also be considered how we can obtain continuous quantum mechanics from the discontinuous classical quantities. If you inspect Fig. 7(b) carefully, you will find a discontinuity of the semiclassical density at $\lambda = 1.0$. The discontinuity is an artifact by naive semiclassical approximations in which the pruning effect of the orbits 6, 6′, and 6″ (see Table I) at $\lambda = 1.0$ is not introduced. If we include the higher-order terms of the semiclassical expansion [23,24], we will reproduce continuous quantum quantities from classical mechanics. Conversely speaking, however well the semiclassical density would resemble the quantum one for a parameter value, we cannot conclude that usual semiclassical theories are sufficient to reproduce low-lying eigenstates. Thus, the study of the parameter variation can be used to perform the crucial test in the validity of the semiclassical approximation for the nonintegrable systems as well as the semiclassical analysis of the system.

ACKNOWLEDGMENTS

The author is pleased to express acknowledgment to Dr. M. Toda for continual encouragements and good advice, without which the author could not finish this work. He is grateful to Professor E. Heller, Professor H. Hasegawa, Professor K. Ikeda, Dr. S. Adachi, and Professor K. Nakamura for encouragements and stimulating discussions. He also expresses gratitude to Dr. A. Shudo, Dr. T. Harayama, and Dr. Y. Shimizu for discussion on periodic orbit quantization, and to Dr. M. Sano, Dr. S. Koga, and Professor S. Akiyama for giving me useful information and references on classical periodic orbits. Numerical calculations are partly carried out on NEC supercomputer SX-3/34R in the computer center of the Institute for Molecular Science.

APPENDIX A: ADDITIONAL TERMS OF TRACE FORMULA

According to the semiclassical theory for billiard systems [12], the density of states $d(k^2) = \sum \delta(k_n^2 - k^2)$ has an expression up to the leading order of k,

$$d(k^2) = \frac{1}{2k}\frac{d}{dk}\sum_{N=1}^{\infty}\frac{1}{N\pi}\,\mathrm{Im}\,\mathrm{tr}\hat{Q}(k)^N\Big|_{\mathrm{PO}}, \qquad \text{(A1)}$$

where $\hat{Q}(k)$ is an integral operator appearing in the boundary element method, and $\mathrm{tr}\hat{Q}^N$ is represented by the integral over the boundary points $\mathbf{r}(s_j)$ [12],

$$\mathrm{tr}\hat{Q}(k)^N = \left(\frac{-ik}{2}\right)^N \oint ds_1 \cdots ds_N \times \prod_{j=1}^{N}\left[\cos\phi_{jj+1}\, H_1^{(1)}(kl_{jj+1})\right]. \qquad \text{(A2)}$$

Here, ϕ_{jj+1} is an incident angle of the $(j+1)$th reflecting point, and $l_{jj+1} = |\mathbf{r}(s_{j+1}) - \mathbf{r}(s_j)|$ is the distance between the jth and $(j+1)$th points.

1. Bouncing ball orbits and its repetition

The contribution of the first traversal of the bouncing ball orbit is represented by the following terms:

$$\mathrm{tr}\hat{Q}\Big|_B = \mathrm{tr}\hat{Q}\Big|_l + \mathrm{tr}\hat{Q}\Big|_{l'} + \mathrm{tr}\hat{Q}\Big|_c . \tag{A3}$$

l denotes a reflection on the upper straight segment, and c represents a reflection on the half circle in the same figure. l' represents a trajectory reflected once from the left edge during the reflections on the upper and lower straight boundary.

The first term in the right-hand side (rhs) is a contribution from the continuous family of the neutral periodic orbits. This has the same expression as the Berry-Tabor formula for the integrable systems.

$$\begin{aligned}\mathrm{tr}\hat{Q}\Big|_l &= -\sqrt{\frac{k}{2\pi}}\int_0^l dx \frac{\exp[2ikr-\pi i/4]}{\sqrt{2r}} \times (-1) \\ &= \frac{l}{2}\sqrt{\frac{k}{\pi r}}\exp\left[2ikr-\frac{\pi i}{4}\right].\end{aligned} \tag{A4}$$

The second term in the rhs of (A3) represents the contribution from the special closed trajectory which bounces once on the left edge (*edge contribution*). In this case, we introduce a variable on the line segment $s_1 = x$. Then the length of the trajectory is represented by $l(x) = 2r+x^2/r$. The critical point of the integral in $k \to \infty$ is $x = 0$,

$$\begin{aligned}\mathrm{tr}\hat{Q}\Big|_{l'} &= -\sqrt{\frac{k}{2\pi}}\int_0^l dx \frac{\exp[2ikr+ikx^2/r-\pi i/4]}{\sqrt{2r}} \\ &= \frac{1}{4}\exp[2ikr-\pi i].\end{aligned} \tag{A5}$$

The third term is the contribution from the connecting point between the line segment and the circle.

$$\begin{aligned}\mathrm{tr}\hat{Q}\Big|_c &= -\sqrt{\frac{k}{2\pi}}\int_0^l dx \frac{\exp[2ikr-ikx^2/r-\pi i/4]}{\sqrt{2r}} \times (-1) \\ &= \frac{1}{4}\exp\left[2ikr-\frac{\pi i}{2}\right].\end{aligned} \tag{A6}$$

From these calculations and Eq. (A1), the contribution from the first traversal of the bouncing ball orbits is represented by

$$\begin{aligned}d_B(k^2) = &\frac{2rl}{2\pi\sqrt{4\pi kr}}\cos\left[2kr-\frac{\pi}{4}\right] \\ &+\frac{r}{4\pi k}\cos\left[2kr-\pi\right]+\frac{r}{4\pi k}\cos\left[2kr-\frac{\pi}{2}\right],\end{aligned} \tag{A7}$$

where the first term in the rhs is the Berry-Tabor term appearing in the trace formula for integrable systems and the other terms are the edge contribution, which should be included in the trace formula as the additional terms.

By the same analysis, we obtain the expression for the second traversal,

$$\begin{aligned}\mathrm{tr}\hat{Q}^2\Big|_{B^2} = &\mathrm{tr}\hat{Q}\Big|_{ll} + 2\,\mathrm{tr}\hat{Q}\Big|_{ll'} + \mathrm{tr}\hat{Q}\Big|_{l'l'} + \mathrm{tr}\hat{Q}\Big|_{cc} \\ &+2\,\mathrm{tr}\hat{Q}\Big|_{lc} .\end{aligned} \tag{A8}$$

The first term in the rhs represents the contribution from a continuous family of the bouncing ball orbit. The second and the third terms are the contribution from the left edge, and the fourth and the fifth terms from the connecting point. These are calculated by stationary phase integral and give

$$\begin{aligned}d_{B^2}(k^2) = &\frac{2rl}{2\pi\sqrt{8\pi kr}}\cos\left(4kr-\frac{\pi}{4}\right) \\ &+\frac{4r}{2\pi k}\left(\frac{\ln(1+\sqrt{2})}{4\sqrt{2}\pi}-\frac{1}{4\pi}-\frac{1}{8}\right)\cos 4kr \\ &+\frac{4r}{2\pi k}\,\frac{1}{8\sqrt{2}}\cos\left(4kr-\frac{\pi}{2}\right).\end{aligned} \tag{A9}$$

2. Orbits on the Dirichlet boundary

The important contribution can be found from the lower edge as well as the left edge which is already studied in the preceding subsection,

$$\begin{aligned}\mathrm{tr}\hat{Q}\Big|_{e,e'} = &\sqrt{\frac{k}{4\pi(l+r)}}e^{2ik(l+r)-i\pi/4} \\ &\times\int_0^\infty dx\left[\exp\left(-\frac{ik}{r}x^2\right)\right. \\ &\left.-\exp\left(-\frac{ikl}{l+r}x^2\right)\right].\end{aligned} \tag{A10}$$

The right-hand side is represented by the sum of two terms, the contributions from the trajectory without any reflection on the lower edge and from one with a reflection on the edge. If we include the multiple traversals, the contribution to the density of states is represented by

$$\begin{aligned}d_{e,e'}(k^2) = \frac{2(l+r)}{2\pi k}\sum_n\left[\frac{\cos\left[2nk(l+r)+n\pi/2\right]}{\sqrt{\mathrm{tr}M^n-2}}\right. \\ \left.+\frac{\cos\left[2nk(l+r)+(n-2)\pi/2\right]}{\sqrt{\mathrm{tr}M^n+2}}\right]\times\frac{1}{2},\end{aligned} \tag{A11}$$

where $\mathrm{tr}M^n = u^n + u^{-n}$, $u = \left[2l+r+2\sqrt{l(l+r)}\right]/r$. The additional factor $1/2$ must be introduced in the rhs. The discussion of the symmetry origin of this factor is given in [16].

3. Orbits through corners

The trajectories going on a right angle corner are considered in this subsection. The contribution of the orbits to the density of states can be obtained by the same analysis as the preceding section. For example, the contribution of orbit 5 in Fig. 1(a) is represented by the following expression:

$$\mathrm{tr}\hat{Q} = -\sqrt{\frac{k}{2\pi}}\frac{\exp[2(r+\sqrt{r^2+l^2})-i\pi/4]}{\sqrt{2(r+\sqrt{r^2+l^2})}} \times \int_{-\infty}^{\infty} dx\ \exp\left[-\frac{ik\sqrt{r^2+l^2}}{r+\sqrt{r^2+l^2}}x^2\right] = \frac{1}{2(r^2+l^2)^{1/4}}\exp\left[2i(r+\sqrt{r^2+l^2})k-\frac{3\pi i}{2}\right], \tag{A12}$$

where x represents the reflection point on a circle. The density of states by this orbit is obtained as

$$d(k^2) = \frac{1}{2\pi k}\frac{2(r+\sqrt{r^2+l^2})}{2(r^2+l^2)^{1/4}} \times \cos\left[2(r+\sqrt{r^2+l^2})k-\frac{3\pi}{2}\right]. \tag{A13}$$

In this case, we can obtain the Gutzwiller term for this orbit by $\mathrm{tr}M-2=4\sqrt{r^2+l^2}/r$ and $\sigma=11$. This gives the consistent result as the calculation above. Thus, we have only to include the usual Gutzwiller contribution as self-retracing orbits for the orbits through right angle corners.

APPENDIX B: LINE-SHAPE FUNCTIONS FOR FOURIER PEAKS

The definition of the line-shape function $f(x)$ for isolated periodic orbits [Eq. (6) in Sec. II B] is

$$f(x) \equiv \frac{2}{\sqrt{\pi}}\int_0^{\infty}\exp(ixt-t^2)\,dt = e^{-x^2/4}+\frac{2i}{\sqrt{\pi}}\,e^{-x^2/4}\int_0^{x/2}e^{t^2}dt. \tag{B1}$$

The imaginary part has the asymptotic expression for large $|x|$,

$$\mathrm{Im}\,f(x) \approx \frac{2i}{\sqrt{\pi}}\frac{x}{x^2-2}. \tag{B2}$$

The line-shape function $g(x)$ corresponding to bouncing orbits is expressed by

$$g(x) \equiv \frac{2}{\Gamma(3/4)}\int_0^{\infty}\sqrt{t}\,\exp(ixt-t^2)\,dt = e^{-x^2/4}\left\{\Phi\left(-\frac{1}{4},\frac{1}{2};\frac{x^2}{4}\right) + \frac{ix\Gamma(5/4)}{\Gamma(3/4)}\Phi\left(\frac{1}{4},\frac{3}{2};\frac{x^2}{4}\right)\right\}, \tag{B3}$$

where $\Phi(\alpha,\gamma;z)$ is the confluent hypergeometric function. $g(x)$ has the asymptotes for $x\to\infty$,

$$g(\pm x) \approx \frac{\sqrt{\pi}\,e^{\pm 3\pi i/4}}{\Gamma(3/4)}\frac{1}{x^{3/2}}. \tag{B4}$$

[1] A. Einstein, Verh. Dtsch. Phys. Ges. **19**, 82 (1917); L. Brillouin, J. Phys. Radium **7**, 353 (1926); J.B. Keller, Ann. Phys. (N.Y.) **4**, 180 (1958).
[2] E.A. Solov'ev, Sov. Phys. JETP **48**, 635 (1978); R.T. Skodje, F. Borondo, and W.P. Reinhardt, J. Chem. Phys. **82**, 4611 (1985); B.R. Johnson, *ibid.* **83**, 1204 (1985).
[3] D.W. Noid, M.L. Koszykowski, and R.A. Marcus, J. Chem. Phys. **78**, 4018 (1983).
[4] M.C. Gutzwiller, J. Math. Phys. **12**, 343 (1971); Physica D **5**, 183 (1982).
[5] P. Cvitanovic and B. Eckhardt, Phys. Rev. Lett. **63**, 823 (1989); M.V. Berry and J.P. Keating, J. Phys. A **23**, 4839 (1990); R. Aurich, C. Matthies, M. Sieber, and F. Steiner, Phys. Rev. Lett. **68**, 1629 (1992).
[6] E.J. Heller, Phys. Rev. Lett. **53**, 1515 (1984).
[7] E.B. Bogomolny, Physica D **31**, 169 (1988); M.V. Berry, Proc. R. Soc. London, Ser. A **423**, 219 (1989).
[8] M. Feingold, R.G. Littlejohn, S.B. Solina, and J.S. Pehling, Phys. Lett. A **146**, 4 (1990); B. Eckhardt, G. Hose, and E. Pollak, Phys. Rev. A **39**, 3776 (1989); D. Wintgen and A. Hönig, Phys. Rev. Lett. **63**, 1467 (1989).
[9] T. Takami, Phys. Rev. Lett. **68**, 3371 (1992).
[10] L.A. Bunimovich, Func. Anal. Appl. **8**, 254 (1974); S.W. McDonald and A.N. Kaufman, Phys. Rev. A **37**, 3067 (1988).
[11] M. Sieber, U. Smilansky, S.C. Creagh, and R.G. Littlejohn, J. Phys. A **26**, 6217 (1993).
[12] D. Alonso and P. Gaspard, J. Phys. A **27**, 1599 (1994).
[13] D. Wintgen, Phys. Rev. Lett. **58**, 1589 (1987); A. Shudo and Y. Shimizu, Phys. Rev. A **42**, 6264 (1990).
[14] M.V. Berry and M. Tabor, Proc. R. Soc. London, Ser. A **349**, 101 (1976); M.V. Berry and M. Tabor, J. Phys. A **10**, 371 (1977); R.J. Richens and M.V. Berry, Physica D **2**, 496 (1981).
[15] S.C. Creagh, J.M. Robbins, and R.G. Littlejohn, Phys. Rev. A **42**, 1907 (1990).
[16] J.M. Robbins, Phys. Rev. A **40**, 2128 (1989).
[17] M.V. Berry and M. Wilkinson, Proc. R. Soc. London, Ser. A **392**, 15 (1984); P.W. O'Connor and E.J. Heller, Phys. Rev. Lett. **61**, 2288 (1988).
[18] T. Takami, Prog. Theor. Phys. Suppl. No. **116**, 303 (1994).
[19] W. Lichten, Phys. Rev. **131**, 229 (1963); F.T. Smith, *ibid.* **179**, 111 (1969); C.A. Mead and D.G. Truhlar, J. Chem. Phys. **77**, 6090 (1982); C.A. Mead, *ibid.* **78**, 807 (1983).
[20] K.T. Hansen (unpublished).
[21] S. Akiyama (private communication).
[22] T. Harayama and A. Shudo, J. Phys. A **25**, 4595 (1992).
[23] P. Gaspard (unpublished).
[24] M. Kuś, F. Haake, and D. Delande, Phys. Rev. Lett. **71**, 2167 (1993).

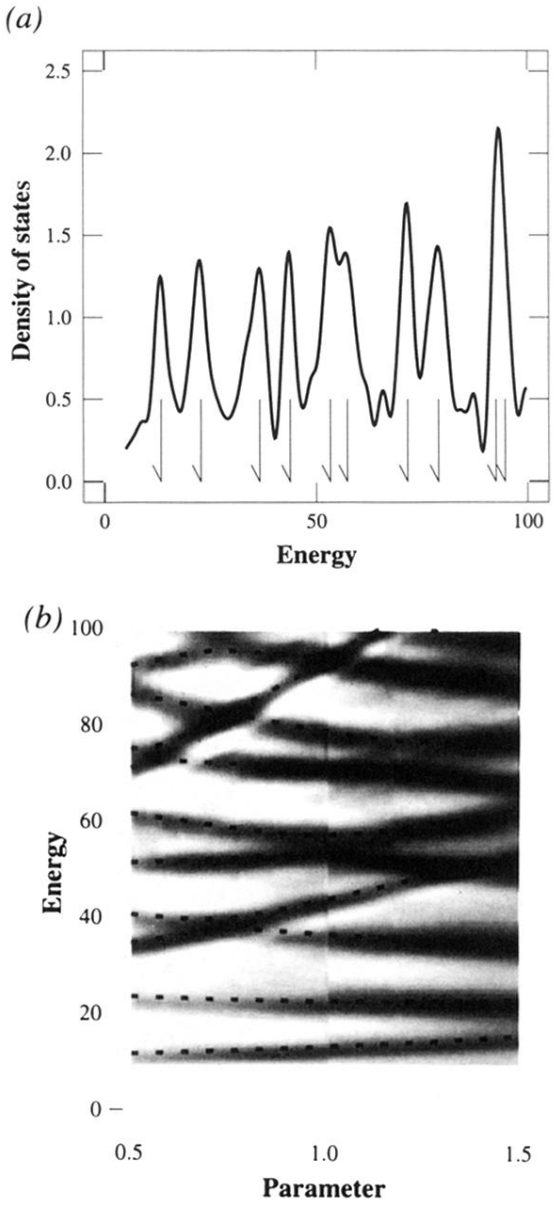

FIG. 7. (a) Semiclassical density of states for $\lambda = 1.0$. (b) Semiclassical density of states as the parameter λ is changed.